

# Lattice-Boltzmann Simulations of Transport Phenomena and Structuring in Suspensions

Jens Harting<sup>1</sup>, Alexander Komnik<sup>1</sup> and Hans J. Herrmann<sup>2</sup>

<sup>1</sup> Institute for Computational Physics, University of Stuttgart,  
Pfaffenwaldring 27, 70569 Stuttgart, Germany

<sup>2</sup> Institute for Building Materials, ETH Höggerberg,  
HIF E 12, 8093 Zürich, Switzerland

## Abstract

We simulate particles suspended in a fluid by means of the lattice-Boltzmann method and its extension to particle suspensions as introduced by Ladd et al. in order to study transport phenomena and structuring effects of particles in the vicinity of sheared rigid walls. We find that a particle free region arises near walls, which has a width depending on the shear rate and the particle concentration. The wall causes the formation of parallel particle layers at low concentrations, where the number of particles per layer decreases with increasing distance to the wall. These findings are in good agreement with a phenomenological theory of Muckenfuß and Buggisch. We also study the velocity distributions of suspended particles which turn out to be non-Gaussian, but exponential.

## 1 Introduction

If one adds a fluid to dry granular materials, the behaviour of the mixture can change dramatically with a host of unexpected phenomena arising. Some common particle-fluid mixtures are ubiquitous in our daily life and include the cacao drink which keeps separating into its constituents, tooth paste and wall paint which are mixtures of finely ground solid ingredients in fluids or blood which is made up of red and white blood cells suspended in a solvent. It is important for industrial applications to obtain a detailed knowledge of those systems in order to optimize production processes or to prevent accidents.

Long-range fluid-mediated hydrodynamic interactions often dictate the behavior of particle-laden flows. A typical example is the objective of the current work: due to external shear forces, a particle concentration gradient orthogonal to the shear plane arises which might generate an overall particle drift orthogonal to the flow direction. This particle drift might cause inhomogeneities in the suspension causing the phenomenon of pseudo wall slip to arise and a particle free region near the wall forms.

Most analytical results for the particle scale be-

havior of suspensions have been obtained for viscous flow ( $Re=0$ ). For large systems, scientists aim at an average, continuum description of the large-scale behavior. However, this requires time-consuming and sometimes very difficult experimental measurements of phenomenological quantities such as the mean settling speed of a suspension, the stress contributions in the system of the individual components (solid and fluid) as functions of, e.g., the solid volume fraction of the constituents.

Computer simulation methods are indispensable for many-particle systems and various simulation methods have been developed to simulate particle-fluid mixtures. All of them have their inherent strengths but also disadvantages. For example, simplified brownian dynamics does not contain long-ranged hydrodynamic interactions among particles at all [17]. Brownian dynamics with full hydrodynamic interactions utilizes a mobility matrix which is based on tensor approximations which are exact in the limit of zero reynolds number and zero particle volume fraction [31, 2]. However, the computational effort scales with the cube of the particle number due to the inversion of matrices. Pair-drag simulations [23] include hy-

hydrodynamic interactions in an approximative way. They have focused on suspensions with high densities (up to 50%) of uncharged spherical colloidal particles. Stokesian dynamics has been presented by Bossis and Brady in the 80s and applied by many authors [12, 1, 38, 18]. However, this method is limited to Reynolds numbers close to zero and the computational effort is very high for dynamical simulations. Even with today's powerful computers it is not possible to study the dynamics of more than a few hundred particles. The method is still widely used due to its physical motivation and its robustness, but is complicated to code. Boundary-element methods are more flexible than Stokesian dynamics and can also be used to simulate non-spherical or deformable particles, but the computational effort is even higher [24, 22]. All these methods assume that hydrodynamic interactions being fully developed and that the dynamics of the fluid and of the solved particles can be treated as fully separated. In reality, this is not the case. Hydrodynamic interactions are time dependent due to local stresses at the fluid-particle interfaces. A number of more recent methods attempt to describe the time dependent long-range hydrodynamics properly with the computational effort scaling linearly with the number of particles. These include recent mesoscopic methods like dissipative particle dynamics [9, 8], the lattice-Boltzmann method [7, 22, 20, 21, 29, 19], or stochastic rotation dynamics [25, 26, 15]. However, for small Reynolds numbers, the computational gain of these methods is lost due to the additional effort needed to describe the fluid motion. Finite element or finite difference methods need a proper meshing of the computational domain which is not trivial for complicated boundary conditions as in the case of dense suspensions. Therefore, many authors only simulated a limited number of static configurations rather than the full dynamics of the system. Advances in remeshing techniques as well as more powerful computers have allowed to overcome these problems. Also, in order to avoid remeshing at all, uniform grids can be used [10, 35]. These methods are flexible and robust. They can properly treat non-Newtonian effects and incorporate inertia, but are complicated to code. For a more detailed description of the simulation methods, experiments or theoretical approaches not addressed in this paper, the reader is referred to one of the various books on colloid science [36, 27, 34, 16].

Here, the lattice Boltzmann method and its exten-

sion to particle suspension as introduced by Ladd is a very good candidate to study the dynamics of glass spheres in a sugar solution [19]. The method is easy to code and has been applied to suspensions of spherical and non-spherical particles by various authors.

For industrial applications, systems with rigid boundaries, e.g., a pipe wall, are of particular interest since structuring effects might occur in the solid fraction of the suspension. Such effects are known from dry granular media resting on a plane surface or gliding down an inclined chute [30, 37]. In addition, the wall causes a demixing of the solid and fluid components which might have an unwanted influence on the properties of the suspension. Near the wall one finds a thin lubrication layer which contains almost no particles and causes a so-called "pseudo wall slip". Due to this slip the suspension can be transported substantially faster and less energy is dissipated.

We expect structuring close to a rigid wall at much smaller concentrations than in granular media because of long-range hydrodynamic interactions. In [19], we study these effects by the means of particle volume concentrations versus distance to the wall. Recently, we have started to study the behavior of particle-laden flows close to a wall in more detail with focussing on the velocity distributions.

## 2 The simulation method

The lattice-Boltzmann method is a simple scheme for simulating the dynamics of fluids. By incorporating solid particles into the model fluid and imposing the correct boundary condition at the solid/fluid interface, colloidal suspensions can be studied. Pioneering work on the development of this method has been done by Ladd et al. [20, 21, 22] and we use their approach to model sheared suspensions near solid walls.

The lattice-Boltzmann (hereafter LB) simulation technique which is based on the well-established connection between the dynamics of a dilute gas and the Navier-Stokes equations [6]. We consider the time evolution of the one-particle velocity distribution function  $n(\vec{r}, \vec{v}, t)$ , which defines the density of particles with velocity  $\vec{v}$  around the space-time point  $(\vec{r}, t)$ . By introducing the assumption of molecular chaos, i.e., that successive binary collisions in a dilute gas are uncorrelated, Boltzmann was able to derive the equation for  $n$  named after

him [6]

$$\partial_t n + \vec{v} \cdot \nabla n = \left( \frac{dn}{dt} \right)_{coll}, \quad (1)$$

where the left hand side describes the change in  $n$  due to collisions. The LB technique arose from the realization that only a small set of discrete velocities is necessary to simulate the Navier-Stokes equations [11]. Much of the kinetic theory of dilute gases can be rewritten in a discretized version. The time evolution of the distribution functions  $n$  is described by a discrete analogue of the Boltzmann equation [22]:

$$n_i(\vec{r} + \vec{c}_i \Delta t, t + \Delta t) = n_i(\vec{r}, t) + \Delta_i(\vec{r}, t), \quad (2)$$

where  $\Delta_i$  is a multi-particle collision term. Here,  $n_i(\vec{r}, t)$  gives the density of particles with velocity  $\vec{c}_i$  at  $(\vec{r}, t)$ . In our simulations, we use 19 different discrete velocities  $\vec{c}_i$ . The hydrodynamic fields, mass density  $\rho$ , momentum density  $\vec{j} = \rho \vec{u}$ , and momentum flux  $\Pi$ , are moments of this velocity distribution  $\rho = \sum_i n_i$ ,  $\vec{j} = \rho \vec{u} = \sum_i n_i \vec{c}_i$ ,  $\Pi = \sum_i n_i \vec{c}_i \vec{c}_i$ . Following the popular approach of Bhatnagar, Gross and Krook, we use a linear collision operator, where the local particle distribution relaxes to an equilibrium state  $n_i^{eq}$  at a single rate  $\tau$  [3]

$$\Delta_i = -\frac{1}{\tau}(n_i - n_i^{eq}). \quad (3)$$

The kinematic viscosity is given by  $\nu = (2\tau - 1)/6$ . To simulate the hydrodynamic interactions between solid particles in suspensions, the lattice-Boltzmann model has to be modified to incorporate the boundary conditions imposed on the fluid by the solid particles. Stationary solid objects are introduced into the model by replacing the usual collision rules (Equation (3)) at a specified set of boundary nodes by the “link-bounce-back” collision rule [29]. Since the velocities in the lattice-Boltzmann model are discrete, boundary conditions for moving suspended particles cannot be implemented directly. Instead, we can modify the density of returning particles in a way that the momentum transferred to the solid is the same as in the continuous velocity case. This is implemented by introducing an additional term  $\Delta_b$  in (2) [20]. To avoid redistributing fluid mass from lattice nodes being covered or uncovered by solids, we allow interior fluid within closed surfaces. Its movement relaxes to the movement of the solid body on much shorter time scales than the characteristic hydrodynamic interaction [20]. If two

particles are in near contact, the fluid flow in the gap cannot be resolved by LB. For particle sizes used in our simulations ( $R < 5a$ ), the lubrication breakdown in the calculation of the hydrodynamic interaction occurs at gaps less than  $0.1R$  [29]. This effect “pushes” particles into each other and can be avoided by applying a lubrication correction method described in [29].

The particle position and velocity is calculated using Newton’s equations

$$\vec{a} = \frac{1}{m} \vec{F} = \dot{\vec{v}}, \quad \vec{v} = \dot{\vec{r}}. \quad (4)$$

The force  $\vec{F}$  is obtained from the calculation of the particle-fluid coupling and the lubrication corrections. Then, the equations are discretized and integrated using the Euler-Cromer method. The velocity  $\vec{v}_{n+1}$  and position  $\vec{r}_{n+1}$  for the time step  $n + 1$  are obtained by utilizing the velocity, position and force from time step  $n$  as well as the time step  $\Delta t = 1$  and particle mass  $m$ .

$$\vec{v}_{n+1} = \vec{v}_n + \frac{\vec{f}_n}{m} \Delta t \quad (5a)$$

$$\vec{r}_{n+1} = \vec{r}_n + \vec{v}_{n+1} \Delta t \quad (5b)$$

The same method is applied to particle rotation, with position replaced by angles, velocity by angular velocity, force by torque and mass by moment of inertia.

### 3 Simulations

The purpose of our simulations is the reproduction of rheological experiments on computers. We simulate a representative volume element of the experimental setup of Buggisch et al. [32, 4, 5, 13, 14] and compare our calculations with experimentally accessible data, i.e., density profiles, time dependence of shear stress and shear rate. We also get experimentally inaccessible data from our simulations like translational and rotational velocity distributions, particle-particle and particle-wall interaction frequencies. The experimental setup consists of a rheoscope with two spherical plates, which distance can be varied. The upper plate can be rotated either by exertion of a constant force or with a constant velocity, while the complementary value is measured simultaneously. The material between the rheoscope plates consist of glass spheres suspended in a sugar-water solution.

The radius of the spheres varies between 75 and  $150\mu\text{m}$ . For our simulations we assume an average particle radius of  $112.5\mu\text{m}$ . The density and viscosity of the sugar solution can also be changed. We simulate only the behavior of a representative volume element which has the experimental separation between walls, but a much lower extension in the other two dimensions than the experiment. In these directions we employ periodic boundary conditions for particles and for the fluid.

Shearing is implemented using the “link-bounce-back” rule with an additional term  $\Delta_{b,i}$  at the wall in the same way as already described for moving particles.

To compare the numerical and experimental results, we need to find characteristic dimensionless quantities of the experiment which then determine the simulation parameters. For this purpose we use the ratio of the rheoscope height and the particle size  $\lambda$ , the particle Reynolds number  $Re$  and the volume fraction of the particles  $\phi$ . The simulation results are provided with units by calculating the length of the lattice constant  $a$  and the duration of one time step as described in [19].

## 4 Results

Figure 1 shows a snapshot of a suspension with 50 spheres after 5772500 time steps which are equivalent to 729 s. Gravity  $\vec{g}$  acts in vertical direction and points to the bottom of the system. The particles feel a gravitational acceleration  $g = 0.8 \text{ m/s}^2$ , have a mass  $m = 7.7 \cdot 10^{-8} \text{ kg}$ , a Reynolds number  $Re = 4.066875 \cdot 10^{-4}$ , and a radius  $R = 1.125 \cdot 10^{-4} \text{ m}$ . The system size is  $1.83 \cdot 10^{-3} \times 1.83 \cdot 10^{-3} \times 3.375 \cdot 10^{-3} \text{ m}$  which corresponds to a lattice size of  $32 \times 32 \times 59$ . The density of the fluid is set to  $\rho_f = 1446 \frac{\text{kg}}{\text{m}^3}$  and its viscosity is  $\eta = 450 \text{ mPa} \cdot \text{s}$ . The walls at the top and the bottom are sheared with a relative velocity  $v_s = 3.375 \cdot 10^{-2} \text{ m/s}$ . Figure 1 is a representative visualization of our simulation data and demonstrates that after the system has reached its steady state, all particles have fallen to the ground due to the influence of the gravitational force. Most of the simulation volume is free of particles.

For a quantitative characterization of structuring effects, we calculate the particle density profile of the system by dividing the whole system into layers parallel to the walls and calculating a partial volume  $V_{ij}$  for each particle  $i$  crossing such a layer  $j$ . The scalar  $V_{ij}$  is given by the volume fraction

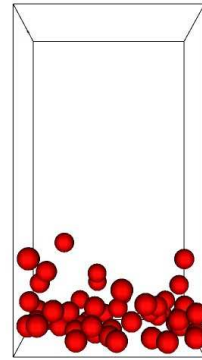


Figure 1: A snapshot of a suspension with 50 spheres. This figure is a typical example of a system that has reached a steady state: all particles have fallen to the ground leaving most of the simulation volume being free of particles [19].

of particle  $i$  that is part of layer  $j$ :

$$V_{ij} = \pi \left( R^2 (R_{ij}^{\max} - R_{ij}^{\min}) - \frac{1}{3} (R_{ij}^{\max} - R_{ij}^{\min}) \right) \quad (6)$$

If the component  $r_{i,z}$  perpendicular to the wall of the radius vector  $\vec{r}_i$  of the center of sphere  $i$  lies between  $r_j^{\min}$  and  $r_j^{\max}$ , we have:

$$r_j^{\min/\max} = (j \mp \frac{1}{2}) \Delta L_z \mp R, \quad (7)$$

$$R_{ij}^{\min/\max} = \begin{cases} \mp R & \text{if } r_{i,z} \mp R < r_j^{\min/\max} \\ r_j^{\min/\max} - r_{i,z} & \text{else} \end{cases}$$

Finally, the sum of all weights associated with a layer is divided by the volume of the layer

$$\phi_j = \frac{1}{L_x \cdot L_y \cdot \Delta L_z} \sum_{i=1}^N v_{ij}, \quad \Delta L_z = \frac{L_z}{M}, \quad (8)$$

with  $L_x, L_y$  being the system dimensions between periodic boundaries,  $L_z$  the distance between walls,  $M$  the number of layers, and  $\Delta L_z$  the width of a single layer.

Density profiles calculated by this means for systems with two different shear rates  $\gamma = 10 \text{ s}^{-1}$  and  $\gamma = 1 \text{ s}^{-1}$  are presented in Fig. 2. All other parameters are equal to the set given in the last paragraph. The peaks in Fig. 2 demonstrate that at certain distances from the wall the number of particles is substantially higher than at other positions. The first peak in both figures is slightly below one particle diameter, which can be explained by a lubricating fluid film between the first layer

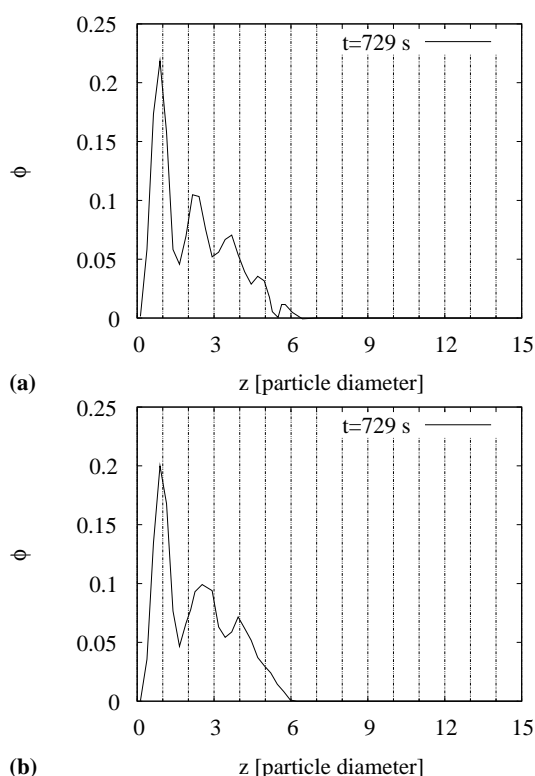


Figure 2: Density profiles from simulations with two different shear rates  $\gamma = 10 \text{ s}^{-1}$  (a) and  $\gamma = 1 \text{ s}^{-1}$  (b) and other parameters being equal to those given in Fig. 1. (a) shows five peaks with separations of about one particle diameter, depicting the formation of particle layers. The number of particles per layer is decreasing with increasing distance to the wall, and the change in particle numbers is caused by gravity which is directed perpendicular to the wall at  $z = 0$ . Although we used the same gravity and particle numbers, there are only three peaks in (b) and their width is higher than in (a), demonstrating that the structuring effects strongly relate to the shear rate.

and the wall which is slightly thinner than one particle radius. Due to the small amount of particles, time dependent fluctuations of the width of the lubricating layer cannot be neglected and a calculation of the exact value is not possible. The five peaks in Fig. 2a have similar distances which are equal to one particle diameter. These peaks can be explained by closely packed parallel layers of particles. Due to the linear velocity profile in  $z$ -direction of the fluid flow, every layer adopts the local velocity of the fluid resulting in a relative velocity difference between two layers of about  $2R\gamma$ . These layers stay stable in time with only a small number of particles being able to be exchanged between them. Figure 2b only shows three peaks with larger distances than in Fig. 2a. However, the average slope of the profile is identical for both shear rates. For smaller shear rates, velocity differences between individual layers are smaller, too.

As a result, particles feel less resistance while moving from one layer to another. Every inter-layer transition distorts the well defined peak structure of the density distribution resulting in only three clearly visible peaks in Fig. 2b. With changing time, the first peak stays constant for both shear rates. The shape, number and position of all other peaks is slightly changing in time. We have com-

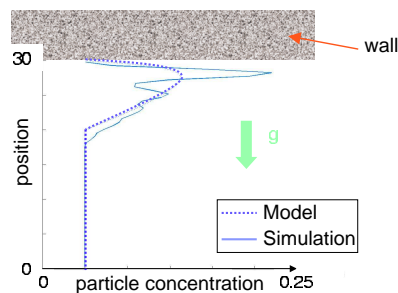


Figure 3: Density profiles from our simulations in comparison to data from the phenomenological theory of Muckenfuß and Buggisch.

pared our results to the phenomenological theory of Muckenfuß and Buggisch [33, 14, 28] as shown in figure 3 and find a good quantitative agreement. We are currently investigating the occurrence of non-Gaussian velocity distributions of particles for higher particle densities and higher shear rates. For this, improvements of the method are mandatory in order to prevent instabilities of the simulation. By utilizing an implicit scheme for the up-

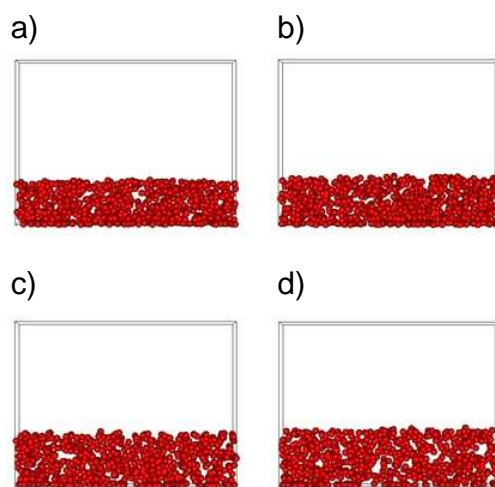


Figure 4: A snapshot of a suspension with 768 spheres after 6.25 million timesteps and varied shear rate used to gain statistics of particle velocity distributions. Shear rates are  $v_s=0.010$  (a),  $v_s=0.014$  (b),  $v_s=0.02$  (c),  $v_s=0.03$  (d) (in lattice units). It can be observed that the height of the occurring sedimentation layer depends on the shear rate.

date of the particle velocities [22, 29] we are able to overcome artefacts caused by numerical inaccuracies at high volume fractions or shear rates. Figure 4 shows snapshots of a system containing 768 particles after 6.25 million timesteps for various shear rates ( $v_s=0.010$  (a),  $v_s=0.014$  (b),  $v_s=0.02$  (c),  $v_s=0.03$  (d)) and a gravitational force of  $-0.72 \cdot 10^{-4}$  (in lattice units). The lattice size is  $80 \times 10 \times 60$  and the upper and lower wall are sheared while all other boundaries are periodic. One can clearly observe a dependence of the height of the sedimentation layer on the shear rate, i.e., with increasing shear rate, the height of the sediment increases. We are interested in the velocity distributions of the particles for different simulation parameters. Figure 5 shows the non-normalized probability distribution function (PDF) for the particle velocities in vertical direction. These distribution functions have been obtained by averaging over all particle velocities at all simulation timesteps. The plots correspond to the snapshots in figure 4. A non-Gaussian behavior of the distributions can be observed, i.e., the tails are exponential and we have shown that they scale as

$$f(v) = A/v_s \cdot \exp(-v/(B \cdot v_s)), \quad (9)$$

where  $v$  denotes the particle velocity and  $A=250$ ,  $B=0.00385$  are constants. A large number of simulations has been performed in order to understand the dependence of the velocity distributions on the simulation parameters. We have not only varied the shear rate, but also the gravitational force and the particle count. It is found that similar laws as given by equation 9 can be found. However, the values for  $A$  and  $B$  do not always stay constant. It is a current matter of investigation to understand the origin of these velocity distributions and the dependence of the fit parameters  $A$  and  $B$  on the simulation parameters.

## 5 Conclusions

We successfully applied the lattice Boltzmann method and its extension to particle suspensions to simulate transport phenomena and structuring effects under shear near solid walls. We adopted the simulation parameters to the experimental setup of Buggisch et al. and are able to obtain not only qualitatively comparable results, but also values that quantitatively correspond to experimentally measured parameters and their phenomenological theory. We have shown that the density profile has

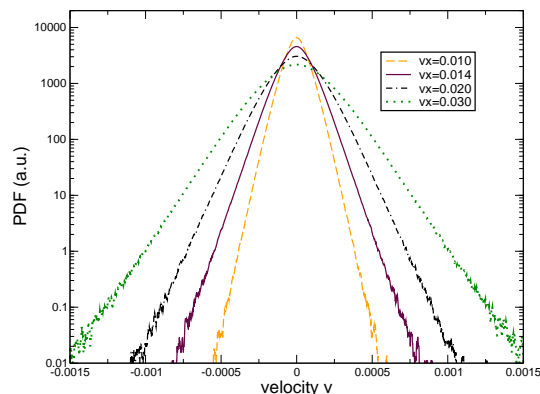


Figure 5: Probability distribution function of the particle velocity in vertical direction. The data corresponds to the snapshots in figure 4. The tails are exponential and follow a law as given by equation 9.

several peaks, confirming the formation of particle layers. We have also shown the occurrence of a “pseudo-wall-slip” of particles, exhibited by a particle free fluid layer near the wall.

The velocity distributions of the particles show exponential tails and we have shown that they scale with the shear rate, gravitational force and the number of particles in the system.

## Acknowledgments

We thank Prof. H.W. Buggisch and S. Muckenfuß for fruitful discussions regarding their experimental setup and for providing the parameters of their experiment. We would also like to thank Prof. A.J.C. Ladd for providing his simulation code.

## References

- [1] A. Sierou and J.F. Brady. Accelerated stokesian dynamics simulations. *J. Fluid Mech.*, 448:115–146, 2001.
- [2] P. Ahlrichs, R. Everaers, and B. Dünweg. Screening of hydrodynamic interactions in semidilute polymer solutions: A computer simulation study. *Phys. Rev. E*, 64(4):040501, 2001.
- [3] P. L. Bhatnagar, E. P. Gross, and M. Krook. Model for collision processes in gases. I. Small amplitude processes in charged and neutral one-component systems. *Phys. Rev.*, 94(3):511–525, 1954.
- [4] H. Buggisch. On mixing and demixing phenomena in granular shear flow. In R. Davis,

- editor, *IUTAM Symposium on Hydrodynamic Diffusion of Suspended Particles*, pages 51–53, 1995.
- [5] H. Buggisch. Plane shear flow with diffusive transport of agglomerates. In *1st International Symposium on Food, Rheology and Structure*, pages 16–20, 1997.
- [6] S. Chapman and T. G. Cowling. *The Mathematical Theory of Non-uniform Gases*. Cambridge University Press, second edition, 1952.
- [7] S. Chen and G. Doolen. Lattice-boltzmann method for fluid flows. *Ann. Rev. Fluid Mech.*, 30:329–364, 1998.
- [8] P. Español. A fluid particle model. *Phys. Rev. E*, 57(3):2390–2948, 1998.
- [9] P. Español and P. Warren. Statistical mechanics of dissipative particle dynamics. *Europhys. Lett.*, 30(4):191–196, 1995.
- [10] A. Fogelson and C. Peskin. A fast numerical method for solving the three-dimensional stokes equations in the presence of suspended particles. *J. Comput. Phys.*, 79:50, 1988.
- [11] U. Frisch, B. Hasslacher, and Y. Pomeau. Lattice-gas automata for the Navier-Stokes equation. *Phys. Rev. Lett.*, 56(14):1505–1508, 1986.
- [12] G. Bossis and J.F. Brady. Dynamic simulation of sheared suspensions. i. general method. *J. Chem. Phys.*, 80(10):5141–5154, 1984.
- [13] H. Buggisch and G. Barthelmes. Possible effects of the diffusion of structural elements on the rheology of shear flows. *Chem. Eng. Tech.*, 21:39–41, 1998.
- [14] H. Buggisch and S. Muckenfuss. Particle concentration in shear flow nearby the wall. *Chem. Eng. Tech.*, 74(7):956–959, 2002.
- [15] M. Hecht, J. Harting, T. Ihle, and H. J. Herrmann. Simulation of claylike colloids. *Physical Review E*, 72:011408, 2005.
- [16] R. J. Hunter. *Foundations of colloid science*. Oxford University Press, 2001.
- [17] M. Hütter. Local structure evolution in particle network formation studied by brownian dynamics simulation. *Journal of Colloid and Interface Science*, 231:337–350, 2000.
- [18] J.F. Brady and G. Bossis. Stokesian dynamics. *Ann. Rev. Fluid Mech.*, 20:111–157, 1988.
- [19] A. Komnik, J. Harting, and H. J. Herrmann. Transport phenomena and structuring in shear flow of suspensions near solid walls. *J. Stat. Mech.: Theor. Exp.*, P12003, 2004.
- [20] A. J. C. Ladd. Numerical simulations of particulate suspensions via a discretized boltzmann equation. part 1. theoretical foundation. *J. Fluid Mech.*, 271:285–309, 1994.
- [21] A. J. C. Ladd. Numerical simulations of particulate suspensions via a discretized boltzmann equation. part 2. numerical results. *J. Fluid Mech.*, 271:311–339, 1994.
- [22] A. J. C. Ladd and R. Verberg. Lattice-boltzmann simulations of particle-fluid suspensions. *J. Stat. Phys.*, 104(5):1191, 2001.
- [23] L.E. Silbert, J.R. Melrose, and R.C. Ball. Colloidal microdynamics: Pair-drag simulations of model-concentrated aggregated systems. *Phys. Rev. E*, 56(6):7067–7077, 1997.
- [24] M. Loewenberg and E. Hinch. Numerical simulation of a concentrated emulsion in shear flow. *J. Fluid. Mech.*, 321:395–419, 1996.
- [25] A. Malevanets and R. Kapral. Mesoscopic model for solvent dynamics. *J. Chem. Phys.*, 110:8605, 1999.
- [26] A. Malevanets and R. Kapral. Solute dynamics in mesoscale solvent. *J. Chem. Phys.*, 112:7260, 2000.
- [27] I. D. Morrison and S. Ross. *Colloidal Dispersions: Suspensions, Emulsions and Foams*. John Wiley and Sons, New York, 2002.
- [28] S. Muckenfuss. *Wall Effects in Shear-Flowing Suspensions*. PhD thesis, University of Karlsruhe, 2006.
- [29] N. Q. Nguyen and A. J. C. Ladd. Lubrication corrections for lattice-boltzmann simulations of particle suspensions. *Phys. Rev. E*, 66(4):046708, 2002.

- [30] P. Mijatović. Bewegung asymmetrischer Teilchen unter stochastischen Kräften. Master-thesis, Universität Stuttgart, 2002.
- [31] D. Petera and M. Muthukumar. Brownian dynamics simulation of bead-rod chains under shear with hydrodynamic interaction. *J. Chem. Phys.*, 111(16):7614–7623, 1999.
- [32] S. Muckenfuß and H. Buggisch. <http://mwww.chemietechnik.uni-dortmund.de/granulare-medien/en/beitrag1.htm>, 2003.
- [33] S. Muckenfuss and H. Buggisch. Shear flow of suspensions under wall influence: Phenomenological theory and effects. *Proc. Appl. Math. Mech.*, 3:414–415, 2003.
- [34] K. S. Schmitz. *Macroions in Solution and Colloidal Suspension*. John Wiley and Sons, New York, 1993.
- [35] S. Schwarzer, K. Höfler, and B. Wachmann. Simulation of hindered settling in bidisperse suspensions of rigid spheres. *Comp. Phys. Comm.*, 268:121–122, 1999.
- [36] D. J. Shaw. *Introduction to Colloid and Surface Chemistry*. Butterworth-Heinemann Ltd, Oxford, 1992.
- [37] T. Pöschel. Granular material flowing down an inclined chute: a molecular dynamics simulation. *J. Phys. II*, 3(1):27–40, 1993.
- [38] T.N. Phung, J.F. Brady, and G. Bossis. Stokesian dynamics simulation of brownian suspensions. *J. Fluid Mech.*, 313:181–207, 1996.